*Electronic supplementary information (ESI)*

*for*

# Complexity of imine and amine Schiff-base tin(II) complexes: drastic differences of amino and pyridyl side arms

Supajittra Yimthachote, Phongnarin Chumsaeng, and Khamphee Phomphrai*

Department of Materials Science and Engineering, School of Molecular Science and Engineering,
Vidyasirimedhi Institute of Science and Technology (VISTEC)
555 Payupnai, Wangchan, Rayong 21210, Thailand.
Email: khamphee.p@vistec.ac.th

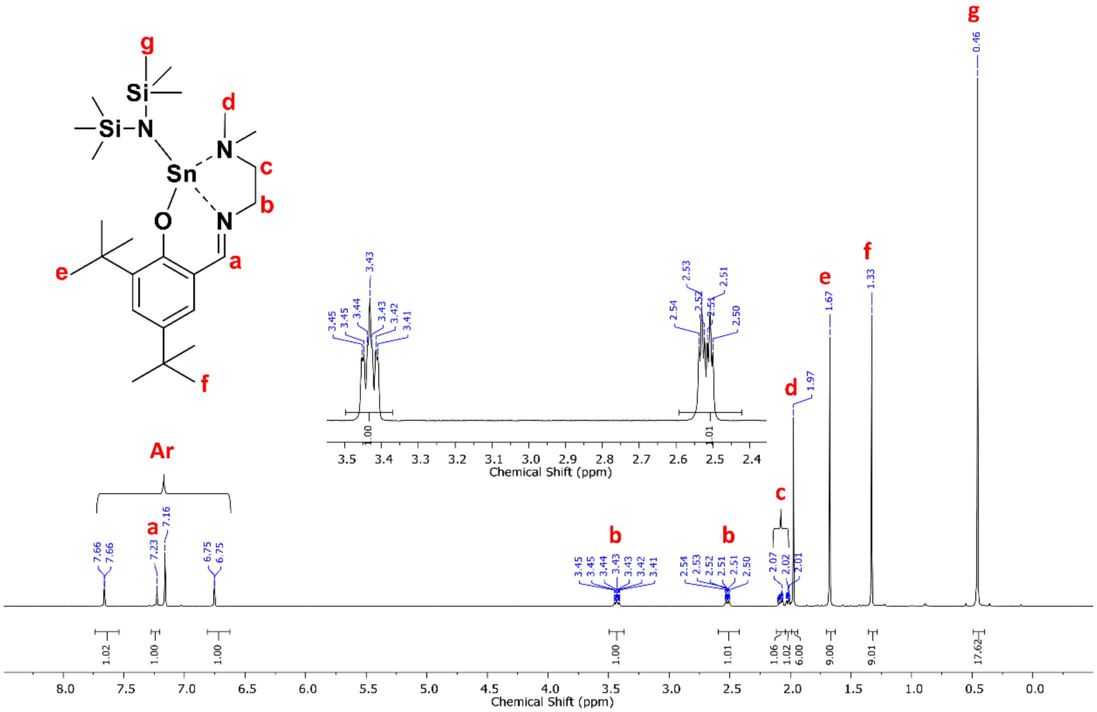

**Figure S1** $^{1}H$-NMR spectrum ($C_6D_6$, 600 MHz, 30°C) of complex **1a**.

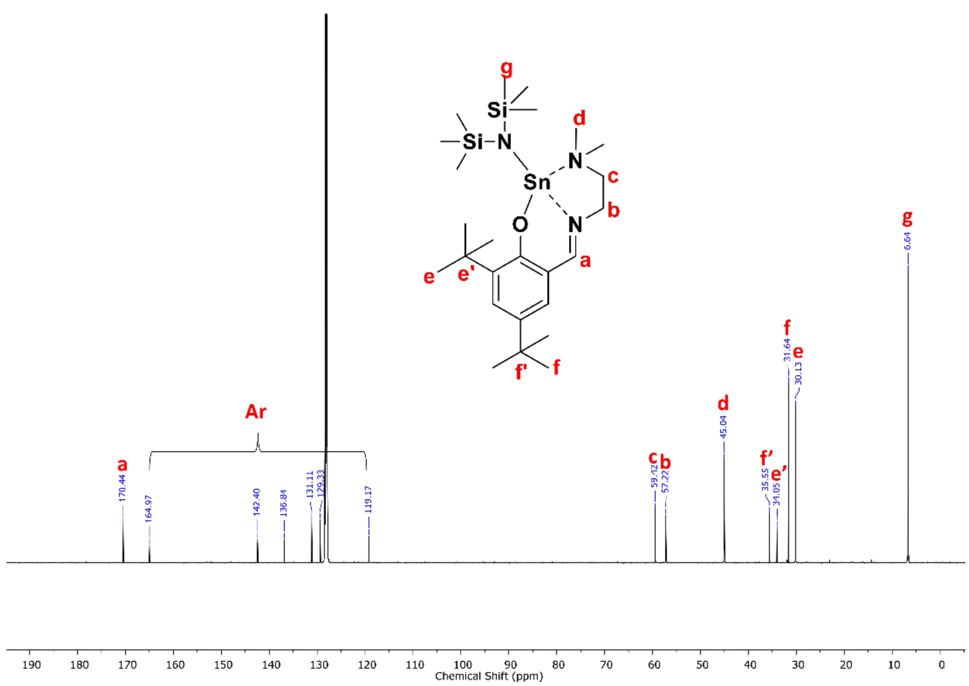

**Figure S2** $^{13}C$-NMR spectrum ($C_6D_6$, 151 MHz, 30°C) of complex **1a**.

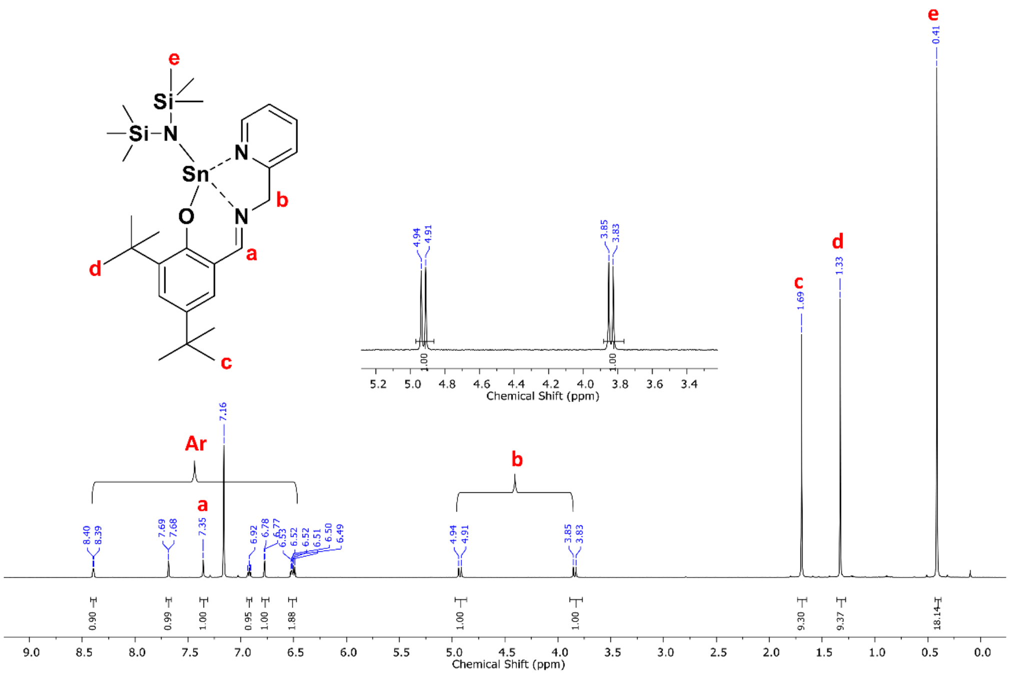


**Figure S3** [1]H-NMR spectrum ($C_6D_6$, 600 MHz, 30°C) of complex **1b**.

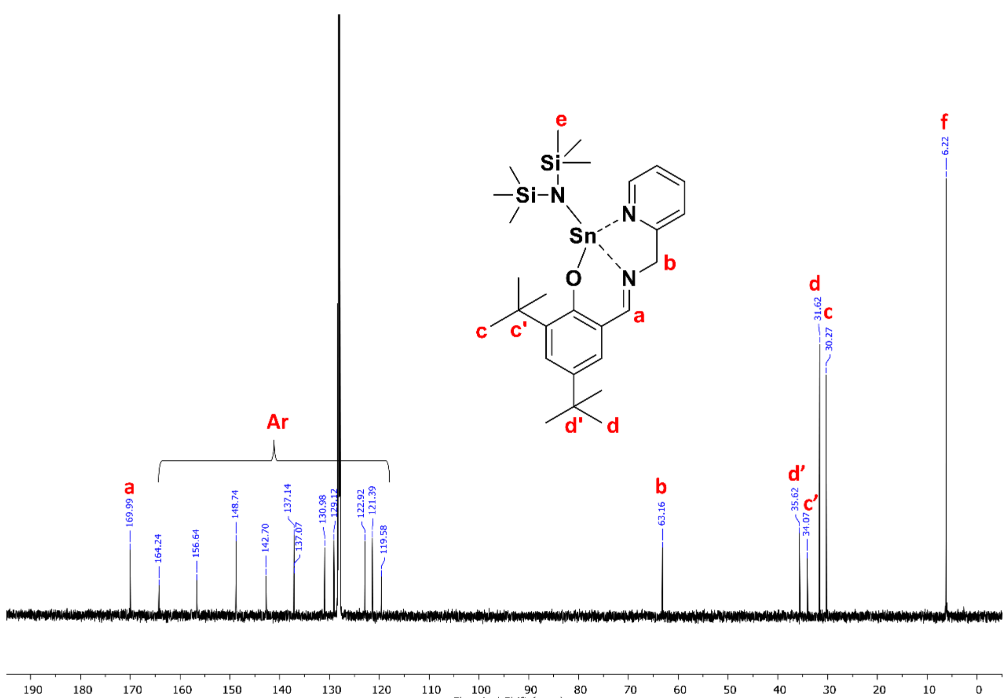


**Figure S4** [13]C-NMR spectrum ($C_6D_6$, 151 MHz, 30°C) of complex **1b**.

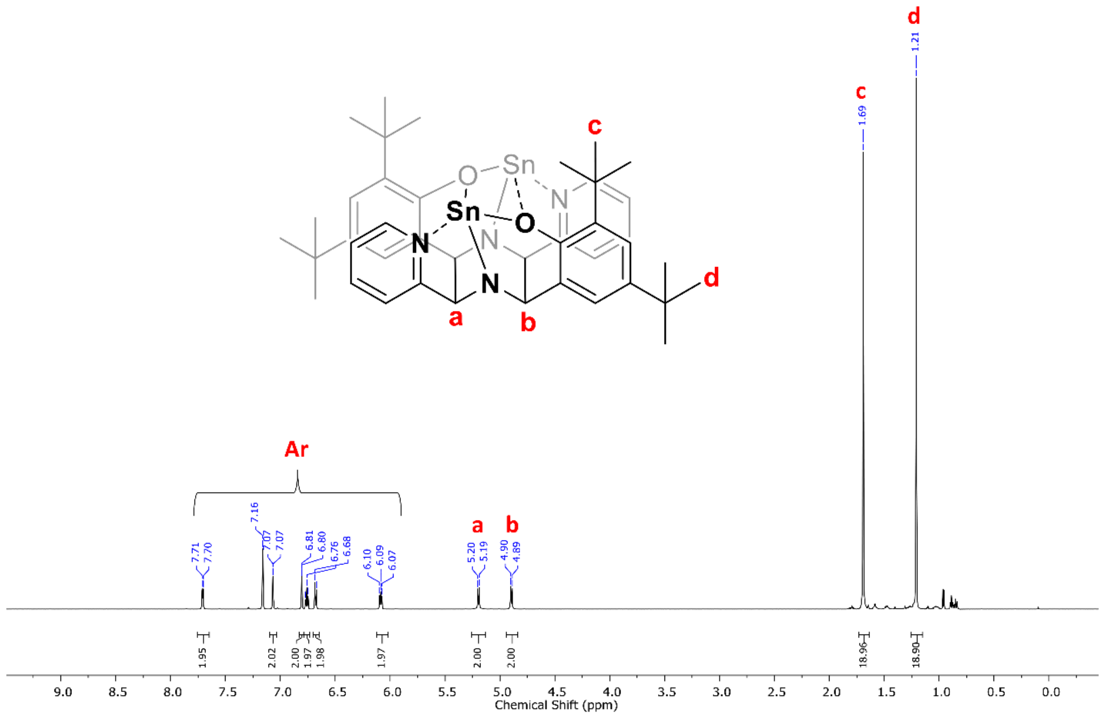


**Figure S5** $^{1}$H-NMR spectrum ($C_6D_6$, 600 MHz, 30°C) of complex **1b’**.

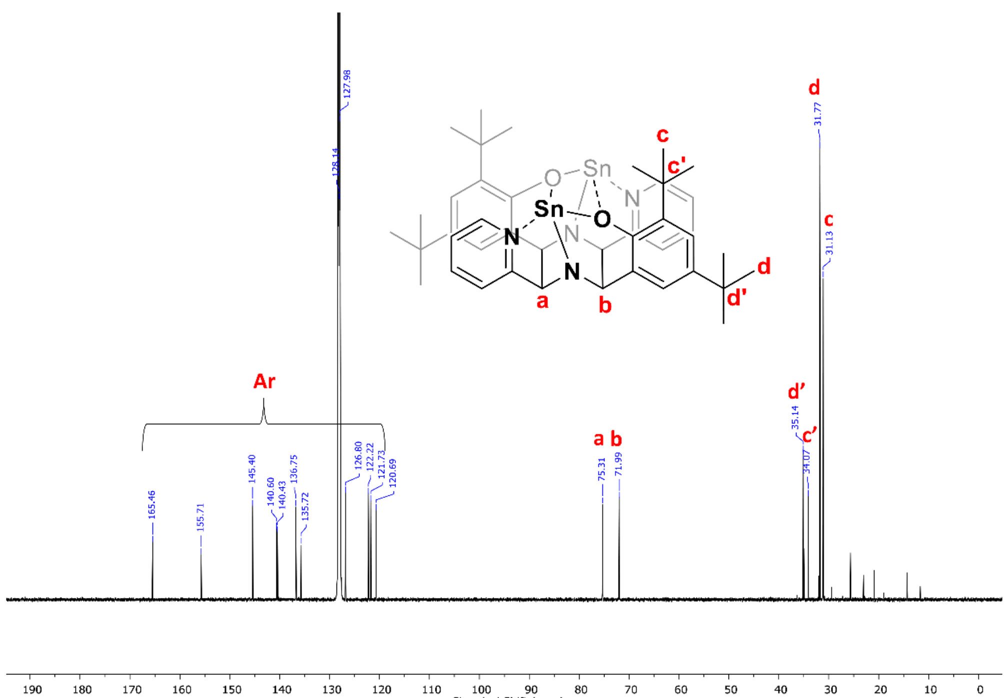


**Figure S6** $^{13}$C-NMR spectrum ($C_6D_6$, 151 MHz, 30°C) of complex **1b’**.

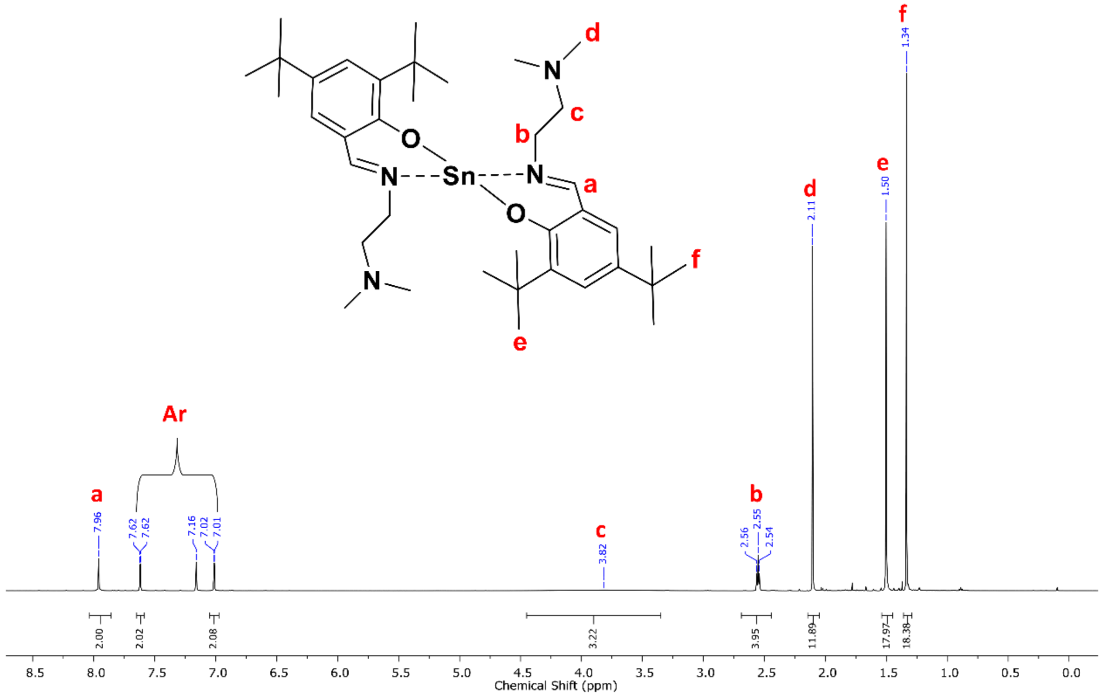

**Figure S7** $^{1}$H-NMR spectrum ($C_6D_6$, 600 MHz, 30°C) of complex **2a**.

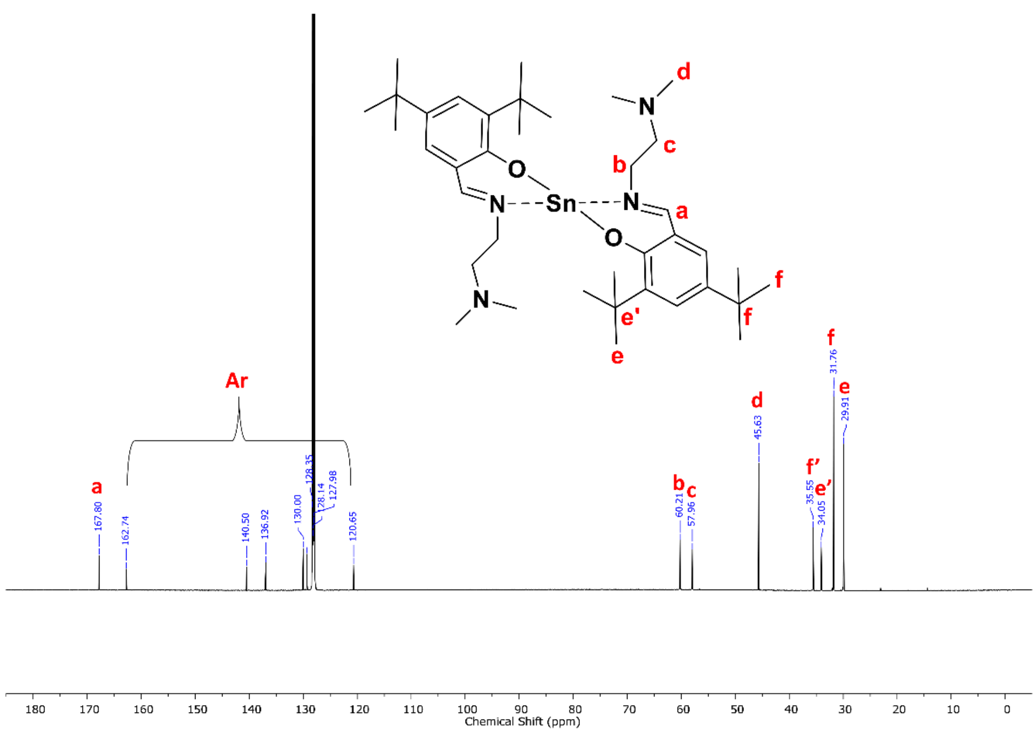

**Figure S8** $^{13}$C-NMR spectrum ($C_6D_6$, 151 MHz, 30°C) of complex **2a**.

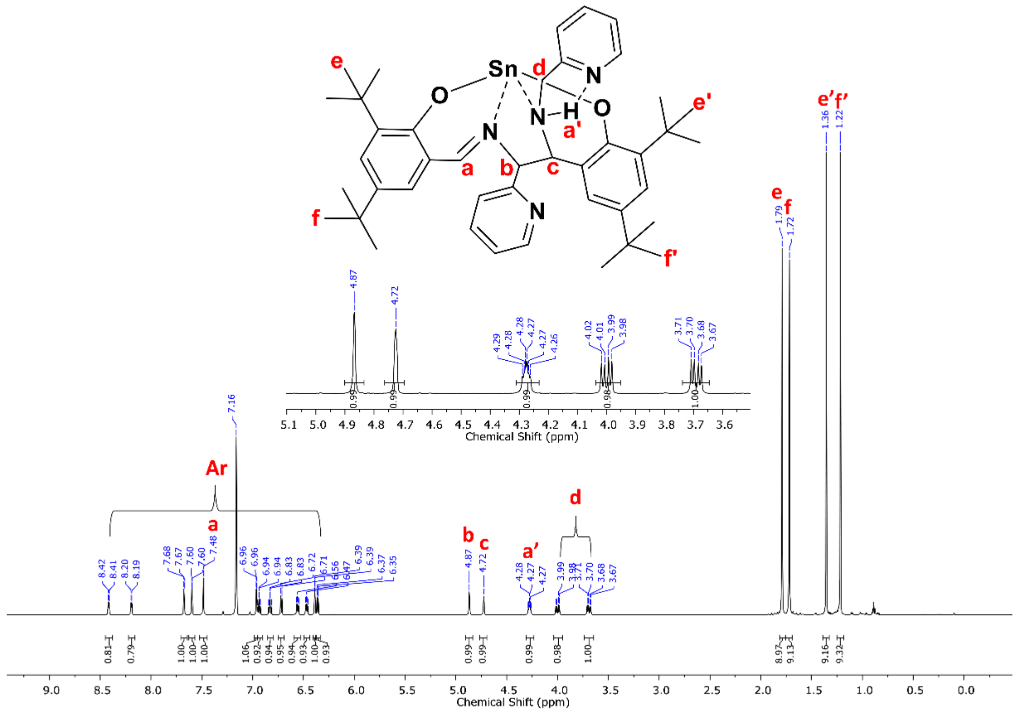


**Figure S9** $^{1}$H-NMR spectrum ($C_6D_6$, 600 MHz, 30°C) of complex **2b’**.

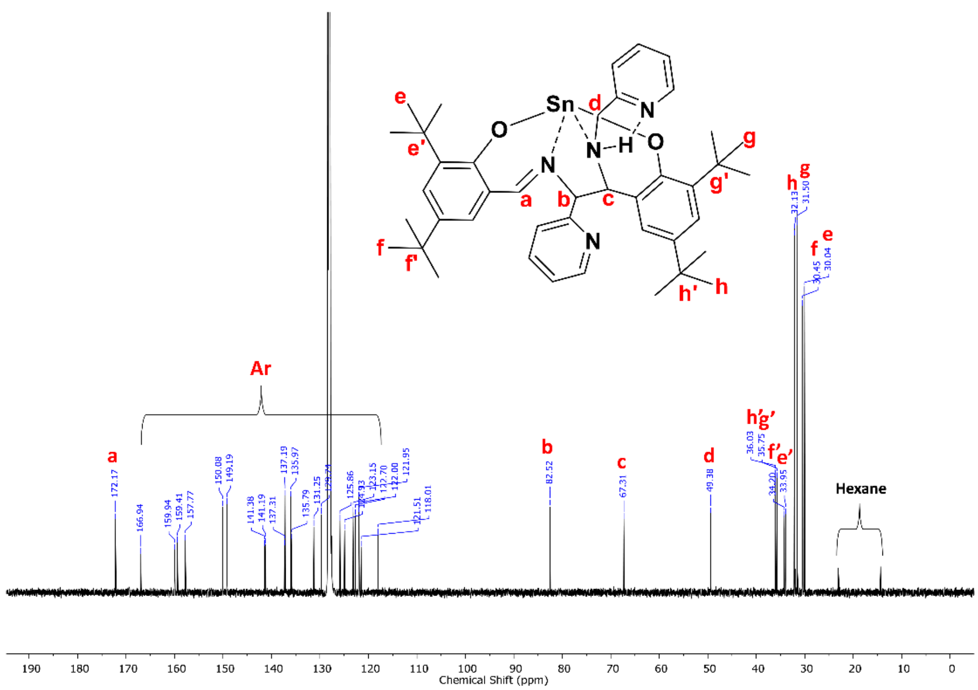


**Figure S10** $^{13}$C-NMR spectrum ($C_6D_6$, 151 MHz, 30°C) of complex **2b’**.

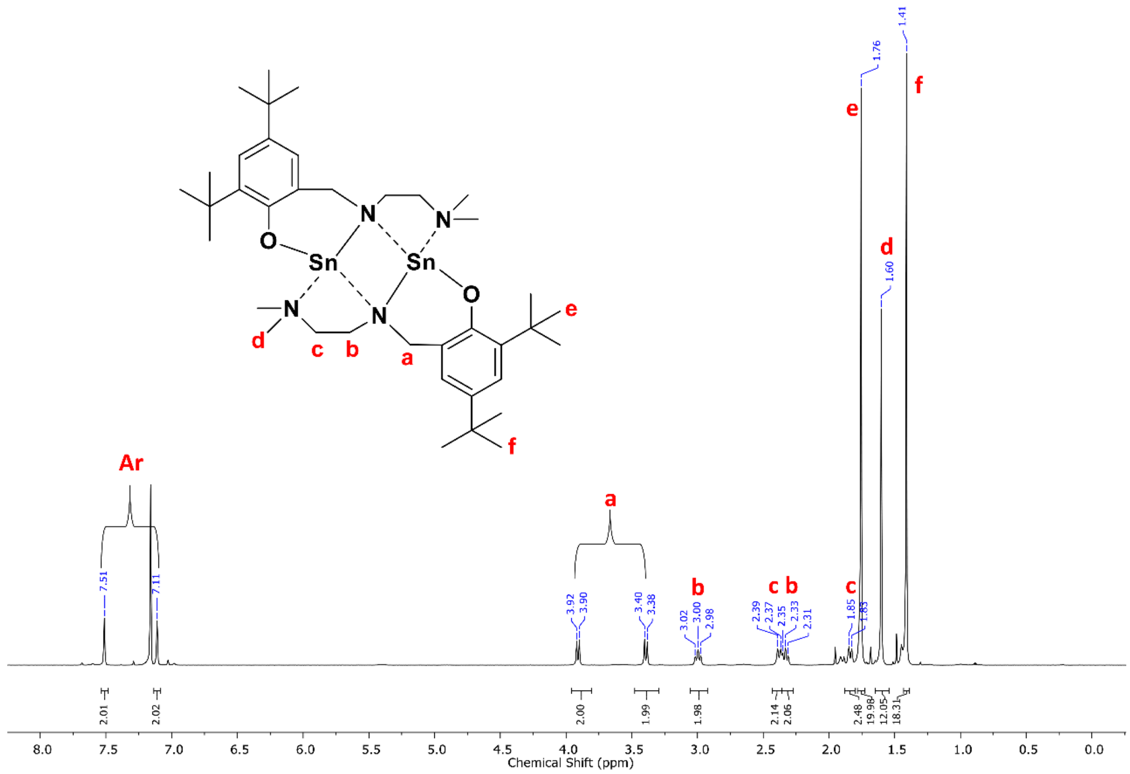

**Figure S11** [1]H-NMR spectrum ($C_6D_6$, 600 MHz, 30°C) of complex **3a**.

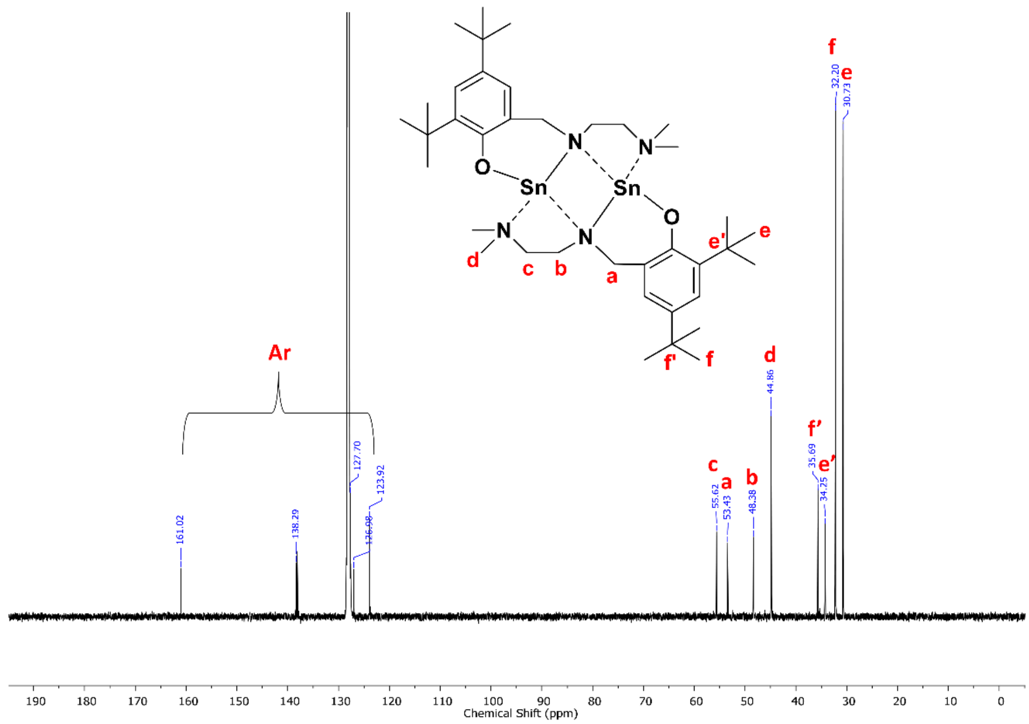

**Figure S12** [13]C-NMR spectrum ($C_6D_6$, 151 MHz, 30°C) of complex **3a**.

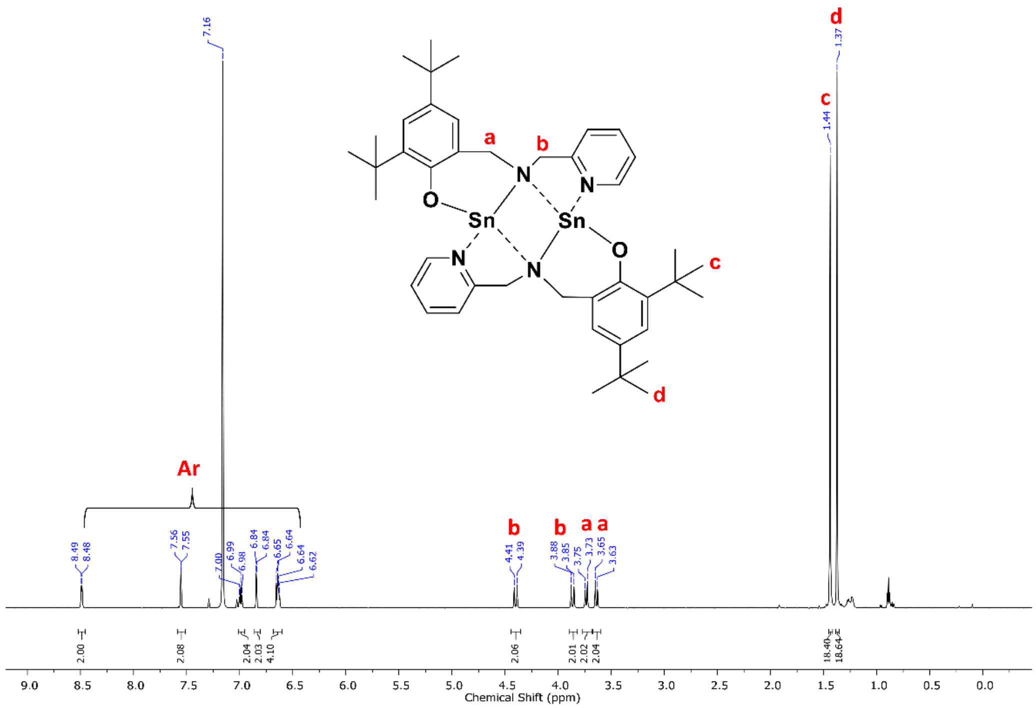

**Figure S13** $^{1}$H-NMR spectrum ($C_6D_6$, 600 MHz, 30°C) of complex **3b**.

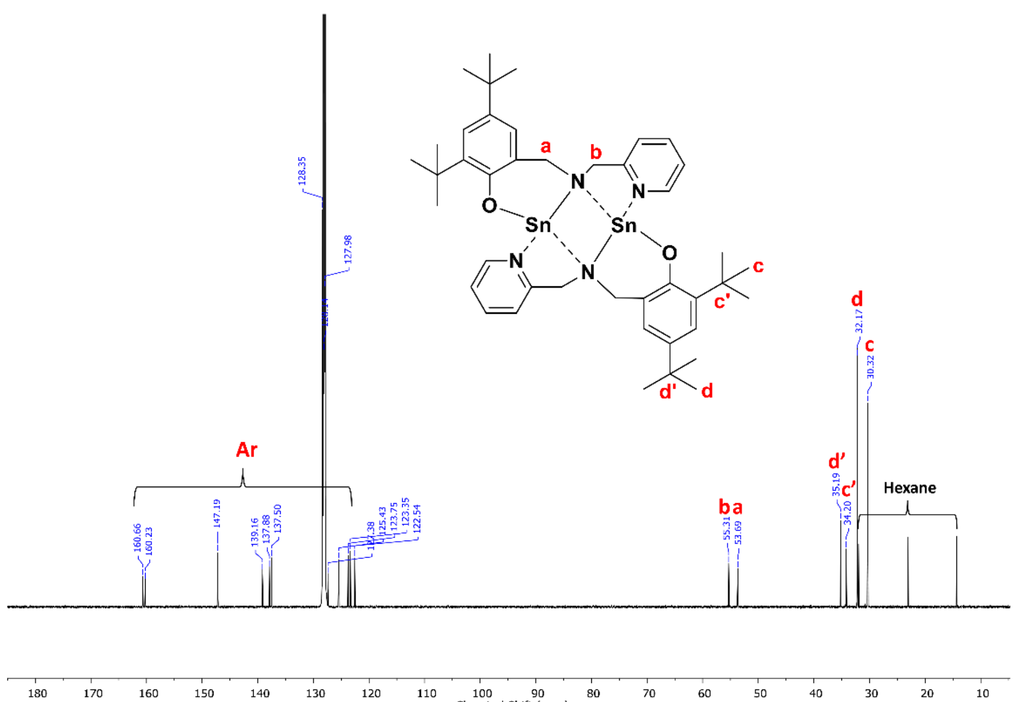

**Figure S14** $^{13}$C-NMR spectrum ($C_6D_6$, 151 MHz, 30°C) of complex **3b**.

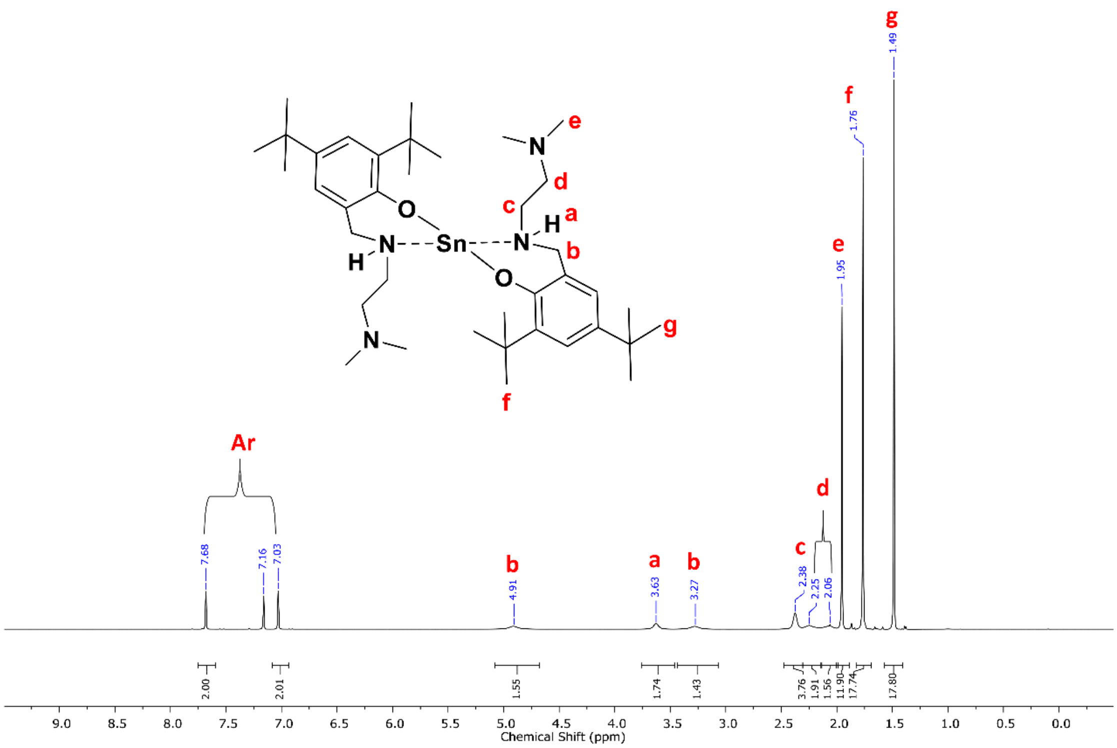


**Figure S15** $^{1}H$-NMR spectrum ($C_6D_6$, 600 MHz, 30°C) of complex **4a**.

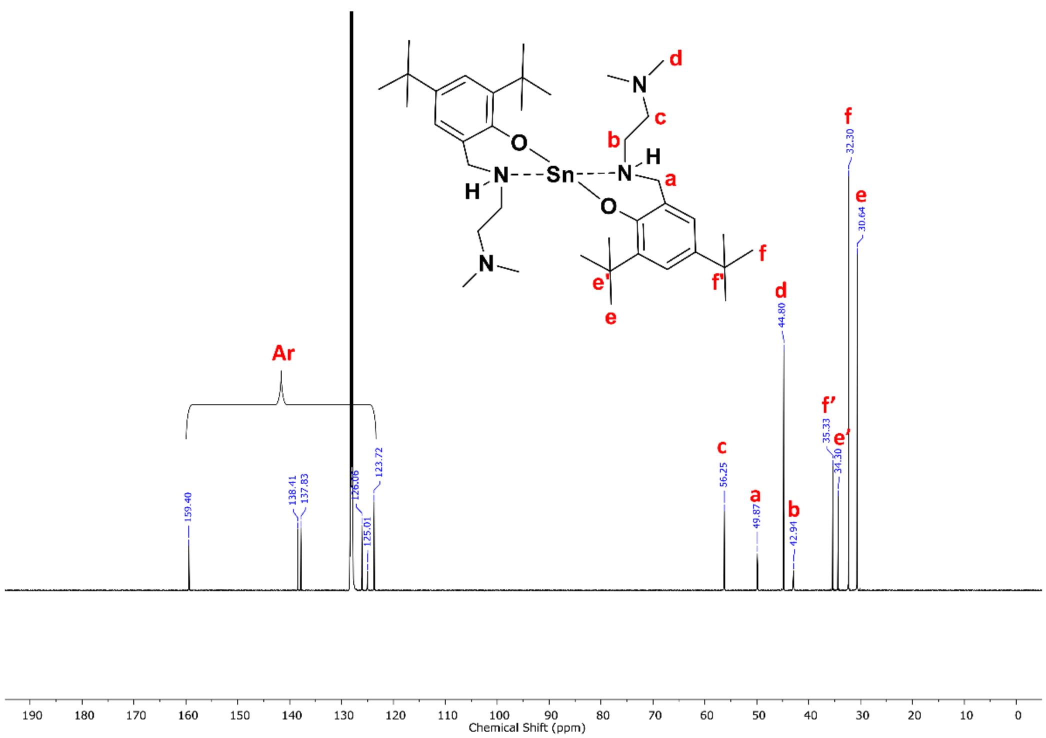


**Figure S16** $^{13}C$-NMR spectrum ($C_6D_6$, 151 MHz, 30°C) of complex **4a**.

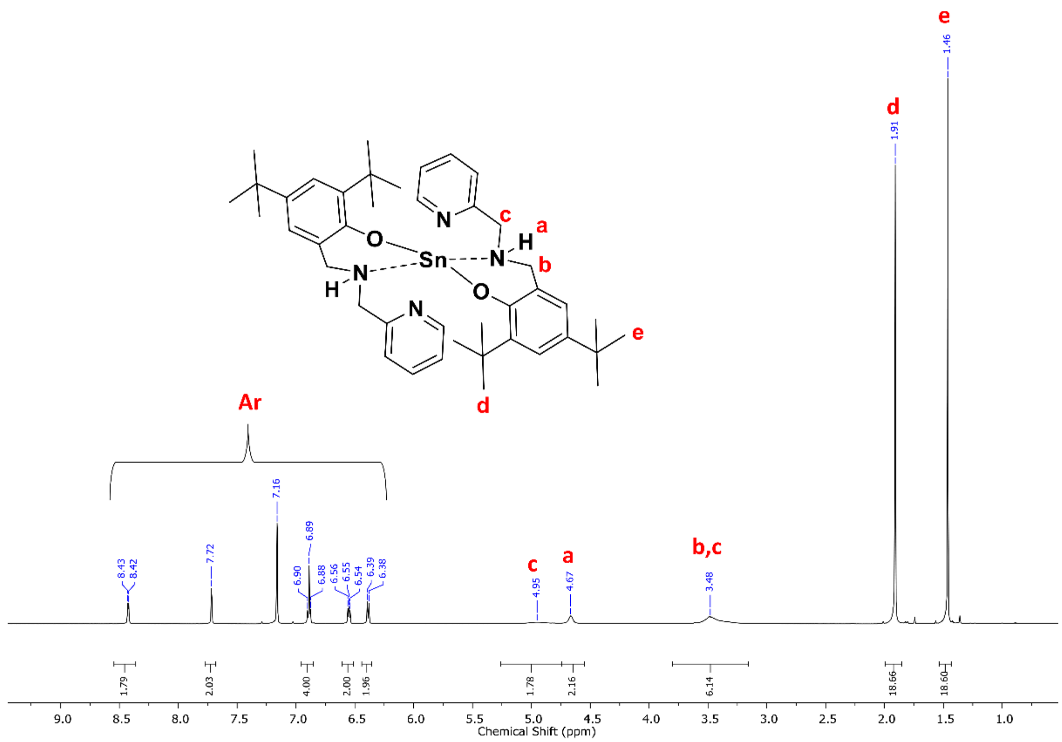


**Figure S17** $^{1}$H-NMR spectrum ($C_6D_6$, 600 MHz, 30°C) of complex **4b**.

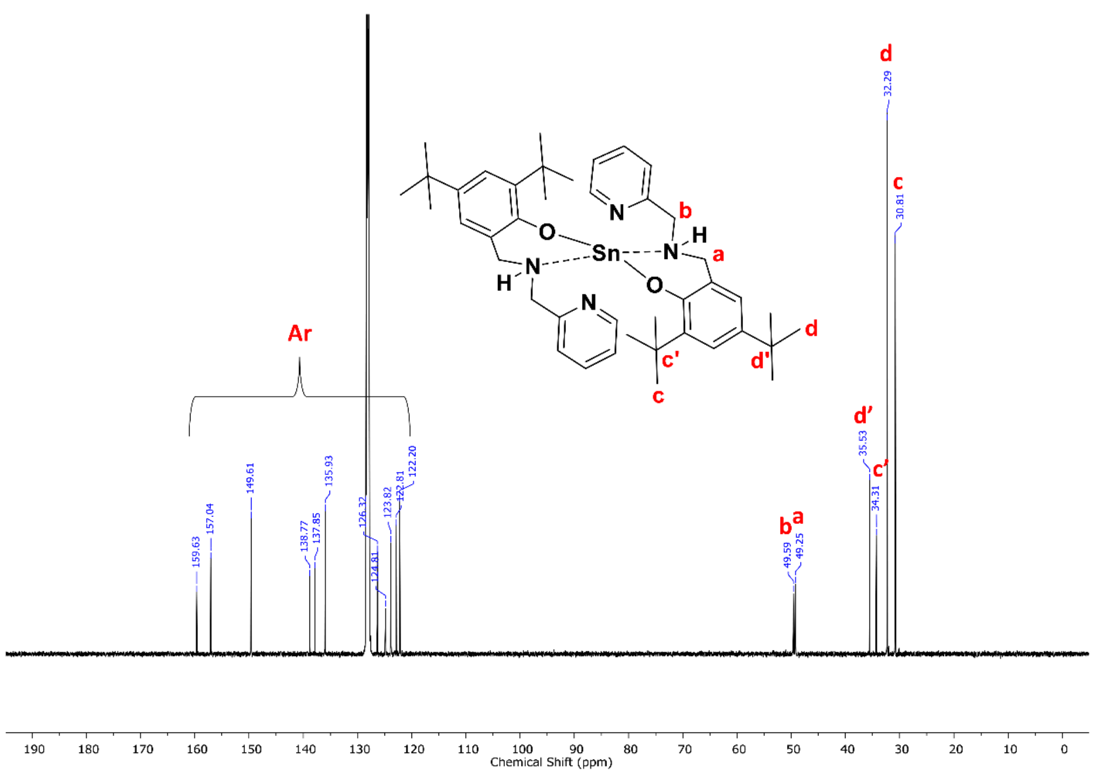


**Figure S18** $^{13}$C-NMR spectrum ($C_6D_6$, 151 MHz, 30°C) of complex **4b**.

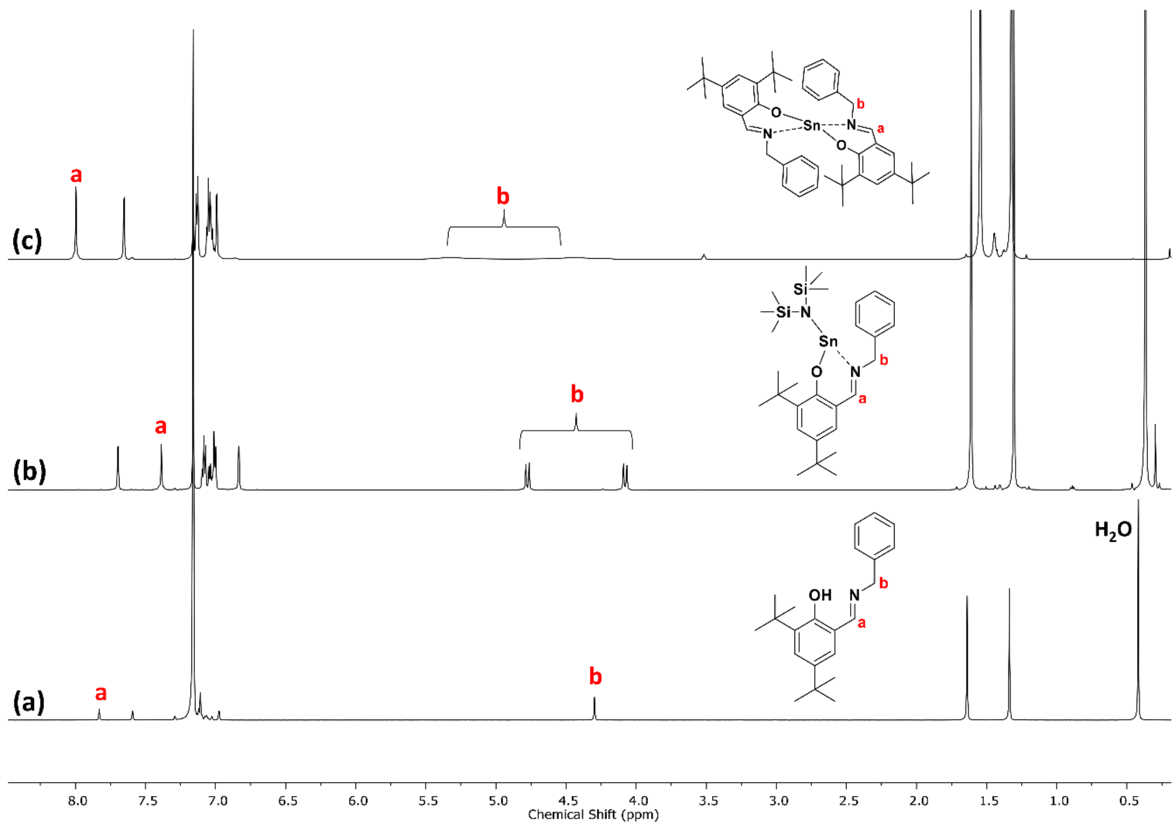


**Figure S19** The NMR-scale reaction ($C_6D_6$, 600 MHz, 30°C) of (a) ligand HL containing N-$CH_2Ph$ moiety, (b) 1:1 reaction of HL and Sn[N($SiMe_3$)$_2$]$_2$ followed by solvent evaporation giving complex LSnN($SiMe_3$)$_2$, and (c) 2:1 reaction of HL and Sn[N($SiMe_3$)$_2$]$_2$ followed by solvent evaporation giving complex $L_2Sn$.

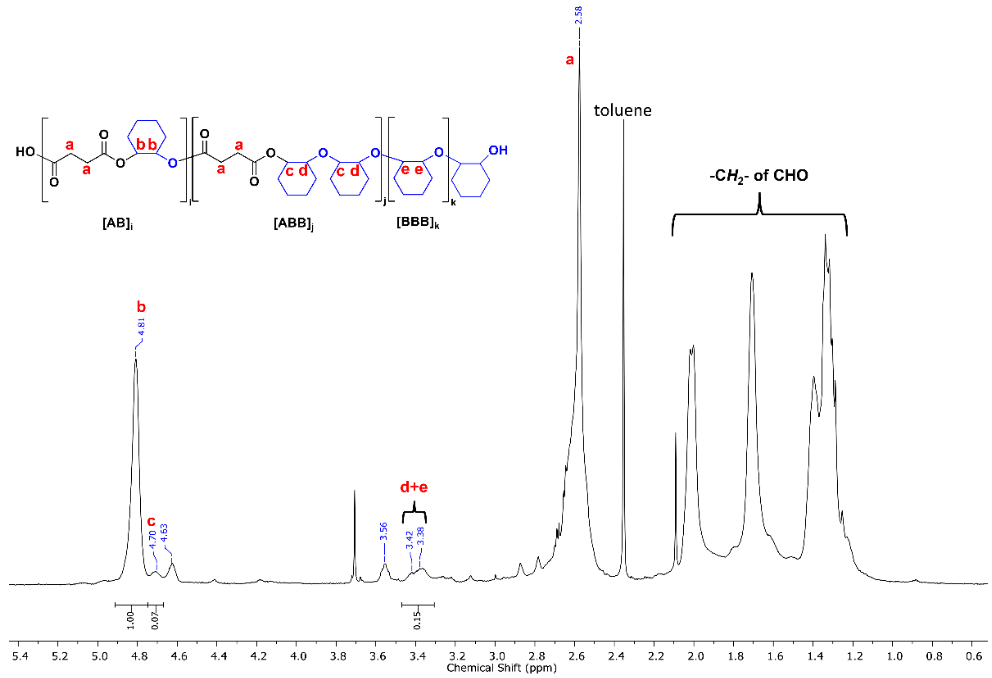


**Figure S20** [1]H-NMR spectrum (600 MHz, $CDCl_3$, 30°C) of the resultant copolymer (Table 1, entry 1) obtained using SA:CHO:**4a** = 50:50:1, $[SA]_0$ = 1.0 M in toluene at 110 °C for 3 h.

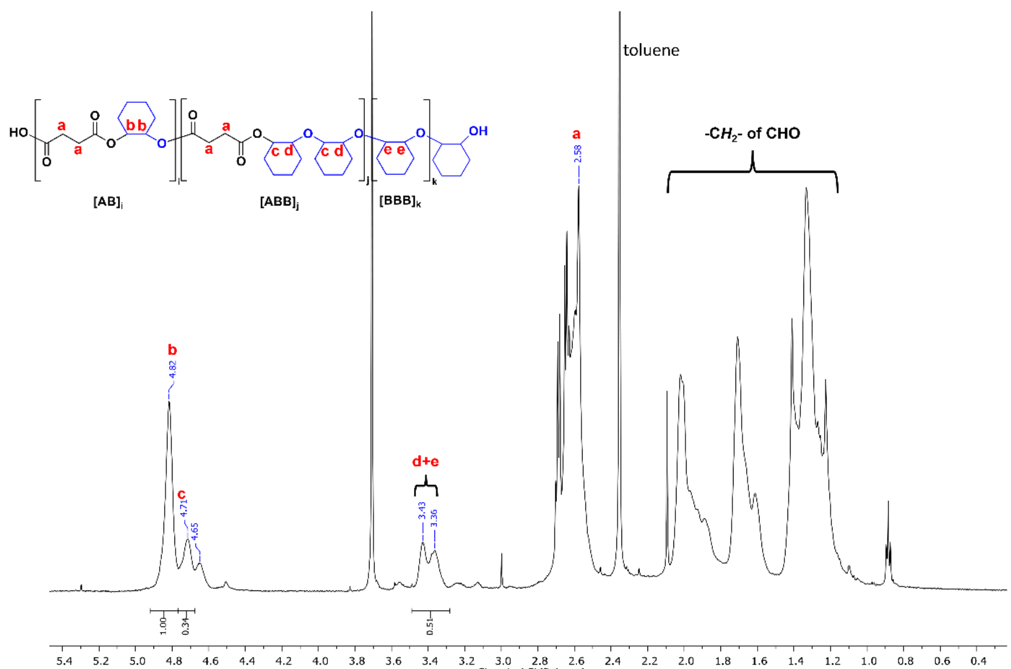


**Figure S21** [1]H-NMR spectrum (600 MHz, $CDCl_3$, 30°C) of the resultant copolymer (Table 1, entry 2) obtained using SA:CHO:**4b** = 50:50:1, $[SA]_0$ = 1.0 M in toluene at 110 °C for 3 h.

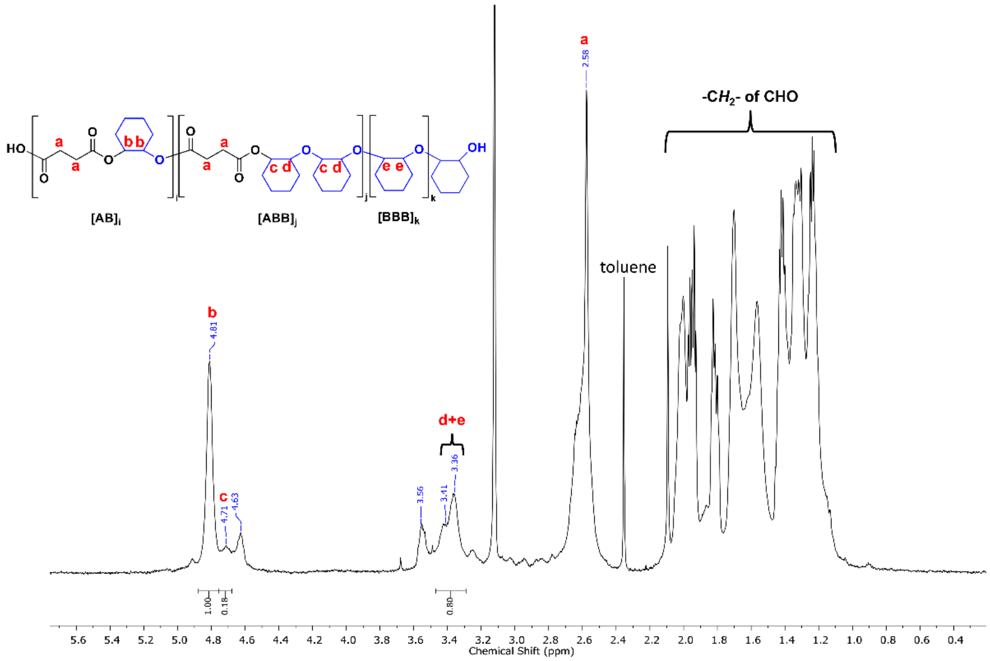


**Figure S22** [1]H-NMR spectrum (600 MHz, $CDCl_3$, 30°C) of the resultant copolymer (Table 1, entry 3) obtained using SA:CHO:**4a** = 50:300:1, $[SA]_0$ = 1.0 M in toluene at 110 °C for 45 min.

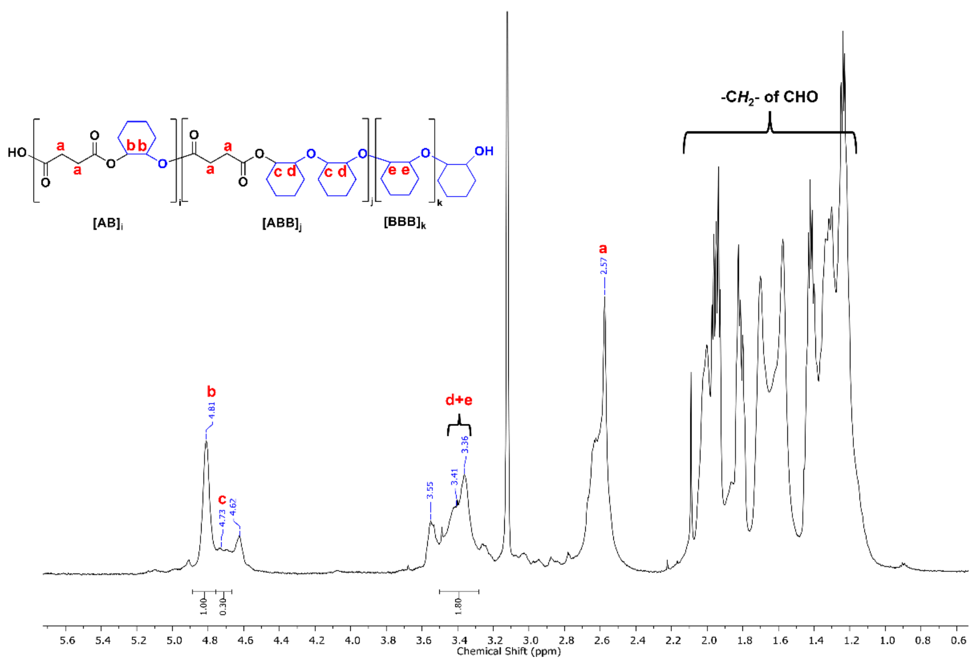


**Figure S23** [1]H-NMR spectrum (600 MHz, $CDCl_3$, 30°C) of the resultant copolymer (Table 1, entry 4) obtained using SA:CHO:**4a** = 50:460:1, neat CHO, at 110 °C for 30 min.

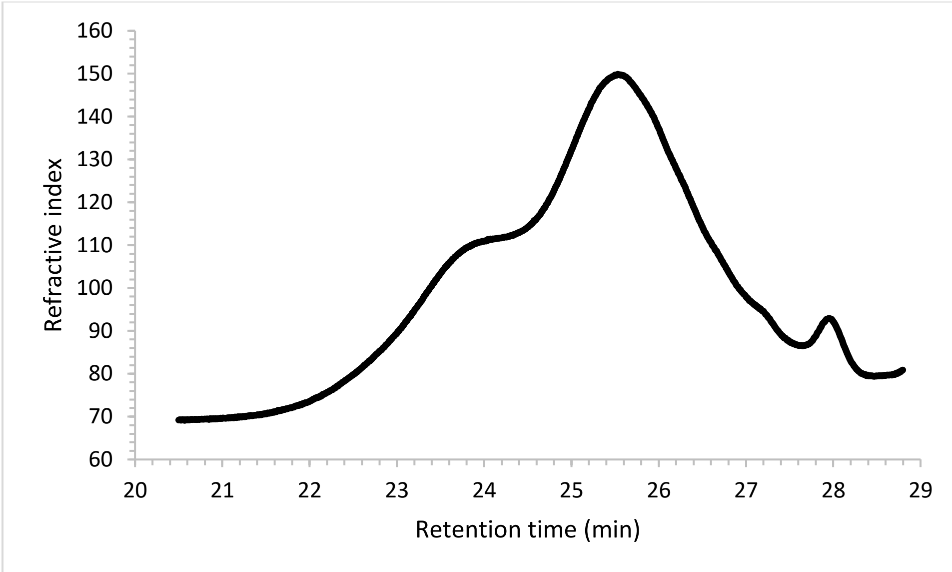


**Figure S24** GPC profile of the resultant copolymer (Table 1, entry 1) obtained using SA:CHO:**4a** = 50:50:1, $[SA]_0$ = 1.0 M in toluene at 110 °C for 3 h.

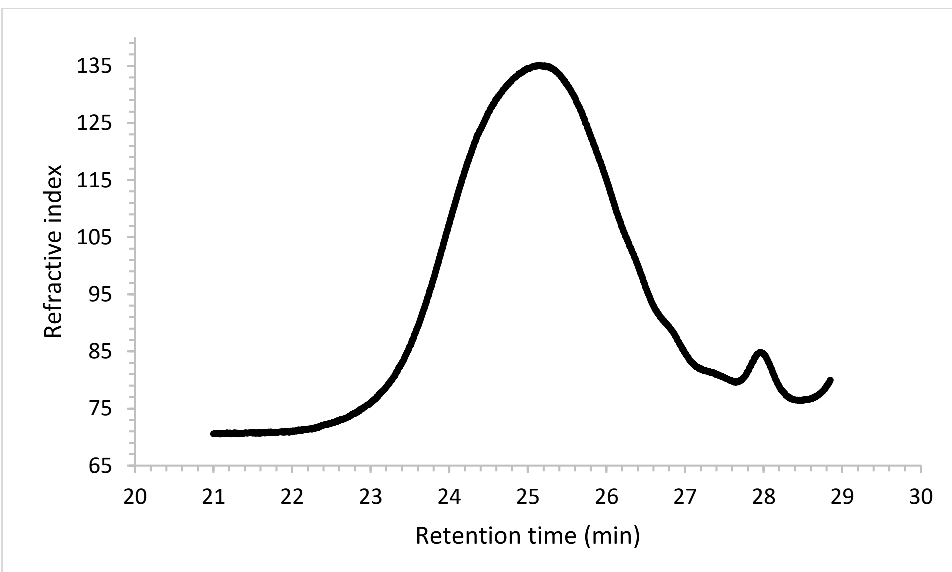


**Figure S25** GPC profile of the resultant copolymer (Table 1, entry 2) obtained using SA:CHO:**4b** = 50:50:1, $[SA]_0$ = 1.0 M in toluene at 110 °C for 3 h.

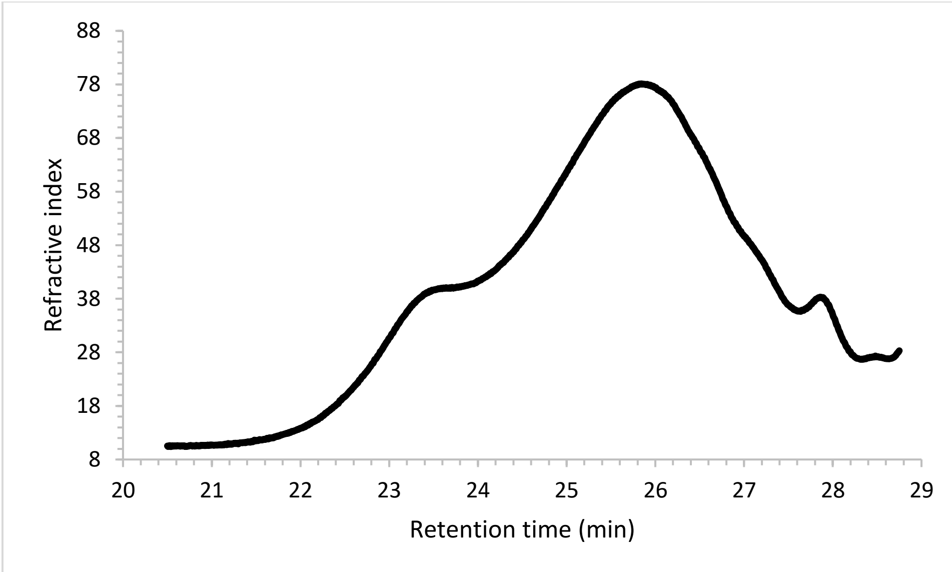


**Figure S26** GPC profile of the resultant copolymer (Table 1, entry 3) obtained using SA:CHO:**4a** = 50:300:1, $[SA]_0$ = 1.0 M in toluene at 110 °C for 45 min.

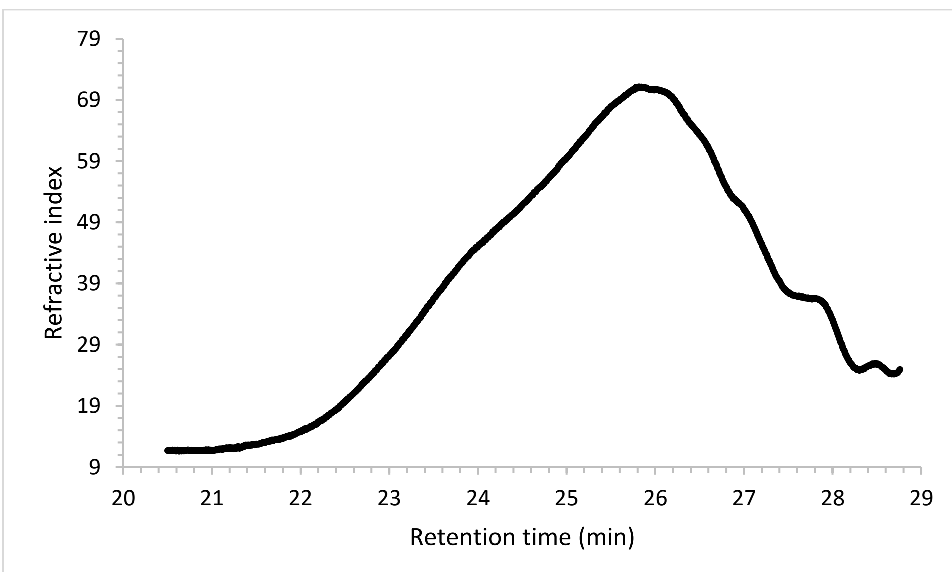


**Figure S27** GPC profile of the resultant copolymer (Table 1, entry 4) obtained using SA:CHO:**4a** = 50:460:1, neat CHO, at 110 °C for 30 min.

## X-ray crystallographic data

**Table S1** Crystals and structure refinement data for complex **1a-4a** and **1b-4b**.

| **Compound** | **1a** | **1b** | **1b'** | **2a** | **2b'** | **3a** | **3b** | **4a** | **4b** |
|---|---|---|---|---|---|---|---|---|---|
| CCDC number | 2102912 | 2102913 | 2102918 | 2102914 | 2102915 | 2102916 | 2102917 | 2102919 | 2102920 |
| Empirical formula | $C_{25}H_{49}N_3OSi_2Sn$ | $C_{27}H_{45}N_3OSi_2Sn$ | $C_{42}H_{52}N_4O_2Sn_2$ | $C_{38}H_{62}N_4O_2Sn$ | $C_{42}H_{54}N_4O_2Sn$ | $C_{38}H_{64}N_4O_2Sn_2$ | $C_{42}H_{56}N_4O_2Sn_2$ | $C_{38}H_{66}N_4O_2Sn$ | $C_{42}H_{58}N_4O_2Sn$ |
| Formula weight | 582.54 | 602.53 | 882.25 | 725.60 | 765.58 | 846.35 | 886.36 | 729.63 | 769.61 |
| Crystal system | Orthorhombic | Monoclinic | Monoclinic | Monoclinic | Monoclinic | Triclinic | Monoclinic | Monoclinic | Monoclinic |
| Space group | $P2_12_12_1$ | $P2_1/n$ | $P2_1/c$ | $C2/c$ | $P2_1/c$ | $P$i | $P2_1/n$ | $P2_1/c$ | $C2/c$ |
| $a$ / Å | 8.489 (1) | 8.332 (1) | 15.635 (2) | 25.758 (2) | 15.197 (1) | 9.063 (1) | 9.571 (1) | 16.287 (1) | 36.251 (3) |
| $b$ / Å | 16.000 (1) | 20.111 (1) | 15.894 (2) | 13.509 (1) | 15.667 (1) | 9.064 (1) | 11.105 (1) | 17.961 (1) | 9.702 (8) |
| $c$ / Å | 22.099 (1) | 18.170 (2) | 18.278 (2) | 24.518 (2) | 19.230 (1) | 13.261 (1) | 21.902 (2) | 14.025 (1) | 25.772 (2) |
| $\alpha$ / ° | 90 | 90 | 90 | 90 | 90 | 71.073 (3) | 90 | 90 | 90 |
| $\beta$ / ° | 90 | 93.329 (4) | 97.412 (4) | 110.166 (3) | 91.923 (3) | 75.736 (3) | 93.592 (3) | 103.863 (2) | 119.231 (3) |
| $\gamma$ / ° | 90 | 90 | 90 | 90 | 90 | 80.550 (3) | 90 | 90 | 90 |
| Cell volume, $V$ / Å$^3$ | 3001.5 (2) | 3039.5 (6) | 4504.2 (9) | 8008.4 (1) | 4575.8 (6) | 994.42 (2) | 2323.4 (4) | 3983.3 (4) | 7910.1 |
| No. of formula units/cell, $Z$ | 4 | 4 | 4 | 8 | 4 | 2 | 2 | 4 | 8 |
| $\rho_{calc.}$/Mg m$^{-3}$ | 1.289 | 1.317 | 1.301 | 1.204 | 1.111 | 1.413 | 1.510 | 1.217 | 1.292 |
| $F$(000) | 1224 | 1256 | 1792 | 3072 | 1600 | 436 | 1072 | 1552 | 3232 |
| Absorption coefficient, $\mu$ / mm$^{-1}$ | 0.951 | 0.942 | 1.144 | 0.672 | 0.592 | 1.291 | 1.344 | 0.676 | 0.685 |
| $T$ / K | 100 | 100 | 100 | 100 | 100 | 100 | 100 | 100 | 100 |
| Crystal color, shape | Yellow, Needle | Yellow-green, Rectangular | Yellow, Rectangular | Yellow, Rectangular | Yellow, Block | Colorless, Rectangular | Yellow, Rectangular | Colorless, Rectangular | Colorless, Prism |
| Crystal size / mm | 0.24 x 0.05 x 0.05 | 0.38 x 0.31 x 0.25 | 0.13 x 0.10 x 0.04 | 0.22 x 0.20 x 0.08 | 0.46 x 0.35 x 0.29 | 0.91 x 0.49 x 0.40 | 0.11 x 0.10 x 0.05 | 0.22 x 0.08 x 0.08 | 0.72 x 0.20 x 0.05 |
| Total no. of reflections measured (not including absences) | 51921 | 139438 | 115240 | 180579 | 70484 | 34131 | 85743 | 133290 | 68140 |
| No. of unique reflections, and $R_{int}$ for equivalents | 5494, 0.0692 | 7251, 0.0245 | 8230, 0.1446 | 11726, 0.0557 | 9007, 0.0349 | 3756, 0.0304 | 6805, 0.0532 | 7834, 0.0403 | 8402, 0.0519 |
| No. of 'observed' reflections [$I > 2\sigma(I)$] | 5189 | 6897 | 6368 | 9872 | 7987 | 3661 | 5803 | 7129 | 6328 |
| Data/restraints/ parameters | 5494/0/303 | 7251/58/347 | 8230/0/463 | 11726/0/428 | 9007/0/455 | 3756/0/216 | 6805/2/278 | 7834/0/422 | 8402/0/463 |
| Goodness-of-fit on $F^2$, S | 1.047 | 1.110 | 1.053 | 1.028 | 1.058 | 1.130 | 1.056 | 1.037 | 1.031 |
| $R$ indices ('observed' data) | $R_1$ = 0.0202, $wR_2$ = 0.0405 | $R_1$ = 0.0204, $wR_2$ = 0.0489 | $R_1$ = 0.0323, $wR_2$ = 0.0697 | $R_1$ = 0.0272, $wR_2$ = 0.0559 | $R_1$ = 0.0225, $wR_2$ = 0.0542 | $R_1$ = 0.0152, $wR_2$ = 0.0396 | $R_1$ = 0.0271, $wR_2$ = 0.0557 | $R_1$ = 0.0197, $wR_2$ = 0.0482 | $R_1$ = 0.0272, $wR_2$ = 0.0582 |
| R indices (all data) | $R_1$ = 0.0236, $wR_2$ = 0.0413 | $R_1$ = 0.0220, $wR_2$ = 0.0505 | $R_1$ = 0.0504, $wR_2$ = 0.0739 | $R_1$ = 0.0393, $wR_2$ = 0.0597 | $R_1$ = 0.0273, $wR_2$ = 0.0560 | $R_1$ = 0.0159, $wR_2$ = 0.0398 | $R_1$ = 0.0379, $wR_2$ = 0.0588 | $R_1$ = 0.0235, $wR_2$ = 0.0498 | $R_1$ = 0.0473, $wR_2$ = 0.0656 |
| Largest diff. peak and hole / eÅ$^{-3}$ | 0.40 and -0.40 | 0.75 and -0.68 | 0.99 and -0.54 | 0.43 and -0.36 | 0.35 and -0.26 | 0.34 and -0.38 | 0.73 and -0.56 | 0.37 and -0.26 | 0.41 and -0.62 |